IEEE Access
Multidisciplinary ⋮ Rapid Review ⋮ Open Access Journal

Received 15 May 2024, accepted 10 July 2024, date of publication 16 July 2024, date of current version 5 August 2024.

Digital Object Identifier 10.1109/ACCESS.2024.3429279

RESEARCH ARTICLE

Numerical Treatment of Non-Linear System for Latently Infected CD4+T Cells: A Swarm-Optimized Neural Network Approach

FARHAD MUHAMMAD RIAZ[1], SHAFIQ AHMAD[2], JUNIAD ALI KHAN[1], SAUD ALTAF[3], ZIA UR REHMAN[4], AND SHUAIB KARIM MEMON[5]

[1]Department of Computer Science, HITEC University, Taxila 47080, Pakistan
[2]Industrial Engineering Department, College of Engineering, King Saud University, Riyadh 11421, Saudi Arabia
[3]Department of Information Engineering Technology, National Skills University Islamabad, Islamabad 44000, Pakistan
[4]Department of Computer Science, National University of Modern Languages (NUML), Islamabad 44000, Pakistan
[5]Department of Computer Science, York St John University, YO31 7EX York, U.K.

Corresponding author: Zia Ur Rehman (zrehman@numl.edu.pk)

This work was supported by King Saud University, Riyadh, Saudi Arabia, through the Researchers Supporting Project RSP2024R387.

ABSTRACT Swarm-inspired computing techniques are the best candidates for solving various nonlinear problems. The current study aims to exploit the swarm intelligence technique known as Particle Swarm Optimization (PSO) for the numerical investigation of a nonlinear system of latently infected CD4+T cells. The strength of the Mexican Hat Wavelet (MHW) based unsupervised Feed Forward Artificial Neural Network (FFANN) is used to solve the nonlinear system of latently infected CD4+T cells. The function approximation of unsupervised ANN is used to construct the mathematical model of the latently infected CD4+T cells by defining the error function in the mean square manner. The adjustable parameters called the unknowns of the network are optimized by using the Particle Swarm Optimization (PSO), Nedler Mead Simplex Method (NMSM), and their hybrid PSO-NMSM. The PSO applied for the global optimization of weights aided by the NMSM algorithm for rapid local search. Finally, a Comprehensive Monte Carlo simulation and statistical analysis of the analytical method, numerical Range Kutta (RK) method, ANN optimized with Genetic Algorithm (GA) aided with Sequential Quadratic Programming (SQP) known as GA-SQP, ANN-PSO-SQP and the proposed MHW-HIVFFANN-PSO-NMSM are performed to validate the effectiveness, stability, convergence, and computational complexity of each scheme. It is observed that the proposed MHW-FFANN-HIVPSO-NMSM scheme has converged in all classes at 10^{-6}, 10^{-7}, and 10^{-8} and solved the nonlinear system of latently infected CD4+ T cells more accurately and effectively. The absolute error lies in 10^{-3}, 10^{-4}, 10^{-4}, and 10^{-5} for numerical, ANN-GA-SQP, ANN-PSO-SQP, and proposed MHW-ANN-PSO-NMSM respectively. Moreover, the proposed scheme is stable for the large number of independent runs. The values for global statistical indicators' global mean squared error are lies 8.15E-09, 3.25E-10, 4.15E-09, and 3.15E-10 for class X(t), W(t), Y(t), and V(t) respectively whereas the global mean absolute deviation lies in range 7.35E-09, 8.50E-10, 2.10E-10 and 7.10E-09.

INDEX TERMS Mathematical modeling, artificial neural network, hybrid optimization, nonlinear system of latently infected CD4+ T cells, Monte Carlo simulations, ANN-based numerical treatment.

I. INTRODUCTION

HIV is an infectious disease that affects the body's immune system by manipulating the body's liquids and killing the T cells of the body. The forecasting of HIV is challenging in the early stage of the disease. In the recent past many mathematical models have been proposed to forecast and model the dynamics of HIV infections [1], [2]. These mathematical models are nonlinear differential coupled systems and can be solved by using analytical and numerical solvers. These

The associate editor coordinating the review of this manuscript and approving it for publication was Qichun Zhang.

solvers are proven well and solve the nonlinear differential system accurately and effectively but have many limitations. For instance, the Analytical and numerical solvers are not generalized and the computation of these solvers cannot be paralyzed over the parallel system. The numerical solvers work on the discretization of the domain under consideration and assumption to solve complex problems and are not generalized because they cannot be used to solve various problems. Additionally, these models are computationally complex.

During the last decade, ANN-bas numerical solvers optimized with different global, local, and hybrid-based optimized techniques have gained more attention for solving the complex nonlinear systems of various problems like medical viruses, computer viruses, physics, and so forth. In 1998, Lagaris proposed neural network-based models to solve the nonlinear problem by converting the boundary value problem into an optimization problem [3]. The use of an ANN-based solver has many advantages over the numerical solver, for instance, the solution of ANN-based solvers is very close to the analytical solver.

ANN-based solvers provide the generalized solution of nonlinear problems, the computational complexity of ANN-based solvers does not increase with the increase in the sampling points and they can be implemented on parallel architecture. ANN-based numerical solvers can approximate any kind of problem directly without any domain knowledge, an assumption for the solution, and the dataset. The supervised ANN solvers have limitations but the unsupervised ANN-based numerical solvers have proven more promising in solving the complex problems of engineering, medicine, and so forth [4], [5], [6]. Many complex systems of science, engineering, medical viruses, computer viruses, and physics are presented in the form of non-linear differential systems. These systems are used to solve real-time complex problems accurately, ANN-based Numerical solvers are proven to solve these systems accurately and effectively, moreover, the ANN-based numerical solvers are fast and can solve the dynamic system where the input, environment, and conditions are changed in real-time. This makes the ANN-based numerical solver more effective in solving real-time complex problems where the conations and data may change over time [4], [7], [8].

ANN-based solvers are used to solve the nonlinear Lienard differential Model [9], nonlinear complex system of predator pre-model [10], lane Emden Model [11], [12], film flow model [13], mass and heat transfer model [14], short-term hydrothermal coordination [15], large scale system [16], Emden-Fowler problem [17], life Cycle Optimization problem [18], Flierl equations [19], [20], heat condition model [14], [21], Singular Periodic boundary problem [22], prey- Predictive system [10], [23], Smoke Problem [24], nervous stomach model [25], Engineering problems [26], Transport system [27], and the medical industry for instance nonlinear COVID system [28], [29], [30], [31], [32], [33], [34], [35], [36], [37], HIV nonlinear system [38], [39], [40], the nonlinear system for dengue fever [41], [42], [43], [44], [45], hepatitis nonlinear system [46], a system of influenza virus [47], [48], [49], and HBV virus [50].

The unknown of the ANN-based numerical solvers needs to be optimized for a better solution to the nonlinear system. The adjustable weights of the ANN-based solvers can be optimized by swarm-based algorithms, bio-inspired algorithms, local search optimizers, and a Hybrid of these.

The majority of the solvers used bio-inspired GA, Swarm PSO, and Ant Colony Optimization (ACO) as global optimizers along with the SQP and ASA [16], [18], [20]. The ANN-based solvers used the Log sigmoid, Morlet Wavelet (MW), and Mexican Hat Wavelet (MHW) as activation functions [10], [25], [38], [39], [41], [51], [52].

The ANN-based solution optimized with GA-SQP to solve the nonlinear system of latently infected CD4+ T cells is presented in [38]. The authors proposed the ANN-based solver to solve the nonlinear system of latently infected CD4+ T cells. The proposed model performs well in terms of absolute error and stability. The built-in log sigmoid has been used as an activation function. However, the computational complexity and the absolute error of the proposed scheme are not promising furthermore the stability in terms of Global Mean Square Error (GMSE) and Global Mean Absolute Deviation (GMAD) needs to improve.

In the recent past, the MHW-based neural network has been proven well to solve a variety of nonlinear systems [52]. The use of PSO with the Nelder Mead Simplex Method to solve the nonlinear system also needs to be investigated. The use of MHW-ANN optimized with the PSO-NMSM can be a good candidate to solve the nonlinear system of latently infected CD4+ T cells.

In a word, there is a need to investigate alternative ANN-based numerical solvers to solve the nonlinear system of latently infected CD4+ T cells. In this work, a Mexican Hat Wavelet Based Single Layer ANN optimized with PSO-NMSM is proposed to solve the nonlinear system of latently infected CD4+T cells. The primary contributions of the study as compared to the findings of the previous studies are as follows.

- The study proposed the Mexican Hat Wavelet-based Feed Forward Single Layer Artificial Neural Network (MHW-HIVFFADNN) to solve the nonlinear system of latently infected CD4+ T cells.
- The adjustable parameters of the neural network are tuned in a hybrid manner using a swarm-based algorithm PSO aided with NMSM an inferior local search technique called PSO-NMSM.
- To validate the accuracy, convergence, and effectiveness of the proposed scheme, a detailed simulation has been performed using an analytical approach, numerical technique (RK), ANN optimized with GA-SQP [38], and proposed schemes.
- The computational complexity and reliability of the proposed scheme are also analyzed through a large number of independent runs.

The rest of the article is summarized as: section II discusses the mathematical model of CD4+T cells, the mathematical formulation of ANN with the Mexican hat wavelet function, the construction of error error-based fitness function, the optimization procedure, and the performance matrices. Section III narrates the simulation and results while section IV is based on the detailed discussion of the results. Section V is based on the concluding remarks and future work.

II. MATERIALS AND METHODS

A. PROBLEM FORMULATION

HIV nonlinear system of latently infected CD4+ T cells is presented in [38] and expressed in (1).

$$\begin{aligned}
\frac{dX}{dt} &= \mu - dX - \alpha XV \qquad X(0) = I_1,\\
\frac{dW}{dt} &= -(q-1)\alpha XV - eW - \lambda W \qquad W(0) = I_2,\\
\frac{dY}{dt} &= \lambda W - \alpha Y + q\alpha XV \qquad Y(0) = I_3,\\
\frac{dV}{dt} &= -V + kY \qquad V(0) = I_4,
\end{aligned} \tag{1}$$

In the above equation, the variables X, W, Y, and V are Susceptible, Infected, Latently, and Infected classes respectively. I_1, I_2, I_3, and I_4 are the initial conditions whereas the constants, α is the infection rate, λ recovery rate, μ UR of the CD4+T cells, d death ratio for susceptible cells, a death ratio for the improved cell, e infection rate k is the latent rate and the q is the elimination rate.

B. MATHEMATICAL FORMULATION OF ANN

The general form of the Differential Neural Network for the first derivate and nth derivate to formulate the problem is presented in (2)-(3) [17]. The graphical representation of the MHW-based ANN to solve the nonlinear differential equations is presented in (2)-(3) is shown in Figure. 1.

$$\tilde{y}(x) = \sum_{i=1}^{n} (\alpha_i f(w_i x + b_i) \tag{2}$$

$$\frac{d^n \tilde{y}}{dx^n} = \sum_{i=1}^{n} \alpha_i \frac{d^n}{dt^n} f(w_i x + b_i) \tag{3}$$

In the above equations, the parameters α, b, and w are the adjustable parameters of the single-layer feed-forward network. Whereas f is the activation function. The adjustable parameters are optimized by using the swarm-based PSO, local optimizer NMSM, and their hybrid. In this work, the MHW is used as an activation function the mathematical formulation of the activation function is expressed in (5).

C. DESIGN OF MHW-HIVFFANN-PSO-NMSM

The neural network formulation of the system of non-linear differential equations expressed in (1) is represented in (4). The Graphical representation of the flow of the proposed framework is shown in Figure. 2.

$$\frac{d\tilde{X}}{dt} = \mu - d\tilde{X} - \alpha\tilde{X}\tilde{V},\ X(0) = I_1$$

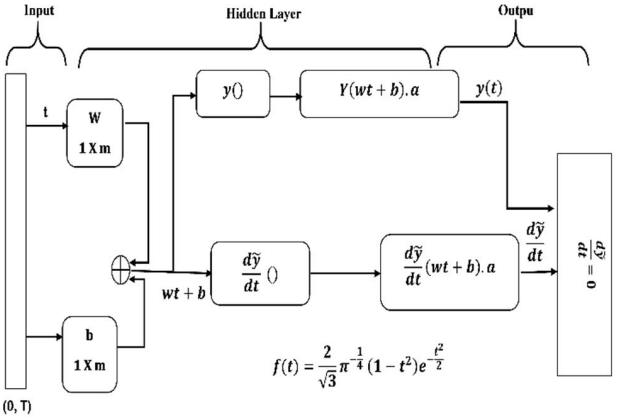

FIGURE 1. Graphical representation of the feed forward MHW artificial neural network.

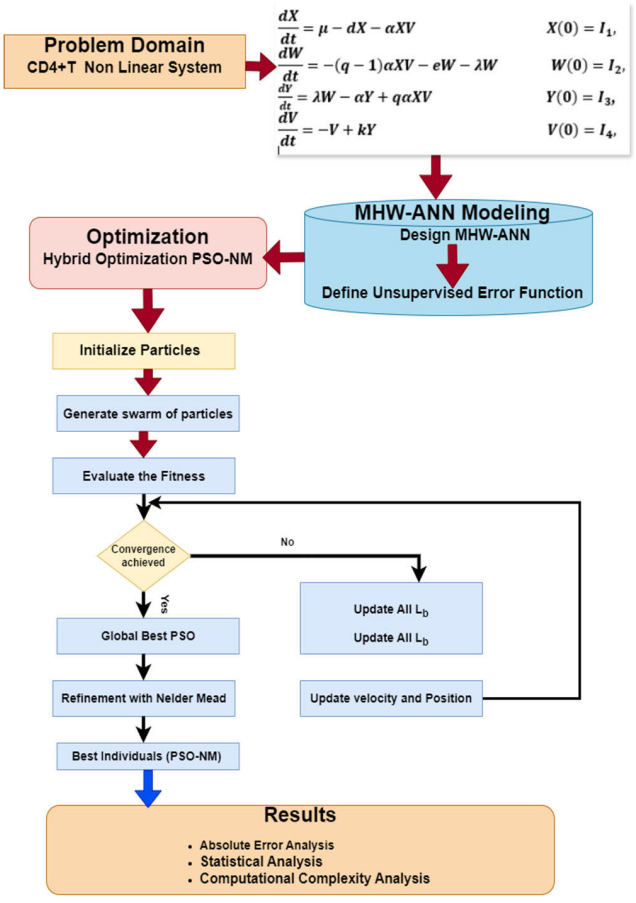

FIGURE 2. Work flow of the proposed technique.

$$\begin{aligned}
\frac{d\tilde{W}}{dt} &= -(q-1)\alpha\tilde{X}\tilde{V} - e\tilde{W} - \lambda\tilde{W},\ W(0) = I_2,\\
\frac{d\tilde{Y}}{dt} &= \lambda\tilde{W} - \alpha\tilde{Y} + q\alpha\tilde{X}\tilde{V},\ Y(0) = I_3,\\
\frac{d\tilde{V}}{dt} &= -\tilde{V} + k\tilde{Y}, V(0) = I_4,
\end{aligned} \tag{4}$$

The mathematical representation of the Mexican Hat Wavelet as an activation function is given by (5).

$$f(\tilde{t}) = \frac{2}{\sqrt{3}}\pi^{-\frac{1}{4}}\left(1-t^2\right)e^{-\frac{t^2}{2}} \tag{5}$$

By applying (5), (4) becomes

$$\begin{aligned}
\frac{d\tilde{X}}{dt} &= \sum_{i=1}^{n}\alpha\tilde{X}_i \\
&\quad\times\left[\frac{2}{\sqrt{3}}\pi^{-0.25}(1-(w\tilde{X}_i t+b\tilde{X}_i)^2)e^{-0.5(w\tilde{X}_i t+b\tilde{X}_i)^2}\right] \\
\frac{d\tilde{W}}{dt} &= \sum\nolimits_{i=1}^{n}\alpha\tilde{W}_i \\
&\quad\times\left[\frac{2}{\sqrt{3}}\pi^{-0.25}(1-(w\tilde{W}_i t+bW_i)^2)e^{-0.5(w\tilde{W}_i t+b\tilde{W}_i)^2}\right] \\
\frac{d\tilde{Y}}{dt} &= \sum_{i=1}^{n}\alpha\tilde{V}_i \\
&\quad\times\left[\frac{2}{\sqrt{3}}\pi^{-0.25}(1-(w\tilde{Y}_i t+bY_i)^2)e^{-0.5(w\tilde{Y}_i t+b\tilde{Y}_i)^2}\right] \\
\frac{d\tilde{V}}{dt} &= \sum_{i=1}^{n}\alpha\tilde{V}_i \\
&\quad\times\left[\frac{2}{\sqrt{3}}\pi^{-0.25}(1-(w\tilde{V}_i t+b\tilde{V}_i)^2)e^{-0.5(w\tilde{V}_i t+b\tilde{V}_i)^2}\right]
\end{aligned} \tag{6}$$

The first derivative of the system of the equation is presented in (7).

$$\begin{aligned}
\frac{d\tilde{X}}{dt} &= \sum_{i=1}^{n}[2\alpha\tilde{X}_i\frac{2}{\sqrt{3}}\pi^{-0.25}e^{-05(b\tilde{X}_i+tw_{\tilde{X}i})^2}w\tilde{X}_i \\
&\quad\times\left(b\tilde{X}_i+tw_{\tilde{X}i}\right)-\alpha_{\tilde{X}i}\frac{2}{\sqrt{3}}\pi^{-0.25}e^{-05(b\tilde{X}_i+tw\tilde{X}_i)^2} \\
&\quad .w\tilde{X}_i(b\tilde{X}_i+tw\tilde{X}_i)(1-(b\tilde{X}_i+tw\tilde{X}_i)^2)] \\
\frac{d\tilde{W}}{dT} &= \sum\nolimits_{i=1}^{n}[2\alpha\tilde{W}_i\frac{2}{\sqrt{3}}\pi^{-0.25}e^{-05(b\tilde{W}_i+tw_{\tilde{W}i})^2}w\tilde{W}_i \\
&\quad\times\left(b\tilde{W}_i+tw_{\tilde{W}i}\right)-\alpha_{\tilde{W}i}\frac{2}{\sqrt{3}}\pi^{-0.25}e^{-05(b\tilde{I}_i+tw\tilde{I}_i)^2} \\
&\quad .w\tilde{W}_i(b\tilde{W}_i+tw\tilde{W}_i)(1-(b\tilde{W}_i+tw\tilde{W}_i)^2)] \\
\frac{d\tilde{Y}}{dT} &= \sum_{i=1}^{n}[2\alpha\tilde{Y}_i\frac{2}{\sqrt{3}}\pi^{-0.25}e^{-05(b\tilde{Y}_i+tw_{\tilde{Y}i})^2}w\tilde{Y}_i \\
&\quad\times\left(b\tilde{Y}_i+tw_{\tilde{Y}i}\right)-\alpha_{\tilde{Y}i}\frac{2}{\sqrt{3}}\pi^{-0.25}e^{-05(b\tilde{Y}_i+tw\tilde{Y}_i)^2} \\
&\quad .w\tilde{Y}_i(b\tilde{Y}_i+tw\tilde{Y}_i)(1-(b\tilde{Y}_i+tw\tilde{Y}_i)^2)] \\
\frac{d\tilde{V}}{dT} &= \sum\nolimits_{i=1}^{n}[2\alpha\tilde{V}_i\frac{2}{\sqrt{3}}\pi^{-0.25}e^{-05(b\tilde{V}_i+tw_{\tilde{V}i})^2}w\tilde{V}_i \\
&\quad\times\left(b\tilde{V}_i+tw_{\tilde{V}i}\right)-\alpha_{\tilde{V}i}\frac{2}{\sqrt{3}}\pi^{-0.25}e^{-05(b\tilde{V}_i+tw\tilde{V}_i)^2} \\
&\quad .w\tilde{V}_i(b\tilde{V}_i+tw\tilde{V}_i)(1-(b\tilde{V}_i+tw\tilde{V}_i)^2)]
\end{aligned} \tag{7}$$

The mathematical formation of the nonlinear system of latently infected CD4+T cells of latently infected cells is presented as follows in (8).

$$\begin{aligned}
&\left[\frac{d\tilde{X}}{dt},\frac{d\tilde{W}}{dt},\frac{d\tilde{Y}}{dt},\frac{d\tilde{V}}{dt}\right] \\
&=\left[\sum\nolimits_{i=1}^{n}\alpha\tilde{X}_i\left[\frac{2}{\sqrt{3}}\pi^{-0.25}\right.\right. \\
&\quad\times\left.(1-(w\tilde{X}_i t+b\tilde{X}_i)^2)e^{-0.5(w\tilde{X}_i t+b\tilde{X}_i)^2}\right], \\
&\quad\times\sum\nolimits_{i=1}^{n}\alpha\tilde{W}_i\left[\frac{2}{\sqrt{3}}\pi^{-0.25}\right. \\
&\quad\times\left.(1-(w\tilde{W}_i t+bW_i)^2)e^{-0.5(w\tilde{W}_i t+b\tilde{W}_i)^2}\right], \\
&\quad\times\sum\nolimits_{i=1}^{n}\alpha\tilde{V}_i\left[\frac{2}{\sqrt{3}}\pi^{-0.25}\right. \\
&\quad\times\left.(1-(w\tilde{Y}_i t+bY_i)^2)e^{-0.5(w\tilde{Y}_i t+b\tilde{Y}_i)^2}\right], \\
&\quad\times\sum\nolimits_{i=1}^{n}\alpha\tilde{V}_i\left[\frac{2}{\sqrt{3}}\pi^{-0.25}\right. \\
&\quad\times\left.\left.(1-(w\tilde{V}_i t+b\tilde{V}_i)^2)e^{-0.5(w\tilde{V}_i t+b\tilde{V}_i)^2}\right]\right]
\end{aligned} \tag{8}$$

The unknowns of the designed Feed Forward single-layer unsupervised neural network are presented as follows

$$Weight\,[w_X,\alpha_X,b_X]=\sum\nolimits_{m=0}^{10}[w_{iX},\alpha_{iX},b_{iX}] \tag{9}$$

$$Weight\,[w_W,\alpha_W,b_W]=\sum\nolimits_{m=0}^{10}[w_{iW},\alpha_{iW},b_{iW}] \tag{10}$$

$$Weight\,[w_Y,\alpha_Y,b_Y]=\sum\nolimits_{m=0}^{10}[w_{iY},\alpha_{iY},b_{iV}] \tag{11}$$

$$Weight\,[w_Y,\alpha_Y,b_Y]=\sum\nolimits_{m=0}^{10}[w_{iY},\alpha_{iY},b_{iV}] \tag{12}$$

The unknown vector W can be presented as

$$W=[W_X,W_W,W_Y,W_V] \tag{13}$$

The parameters of the (13) are expressed as

$$\begin{aligned}
W_X=[w_X,\alpha_X,b_X],\,W_W=[w_W,\alpha_W,b_W],\,W_Y \\
=[w_Y,\alpha_Y,b_Y],\,W_V=[w_V,\alpha_V,b_V]
\end{aligned} \tag{14}$$

The FFANN-based formulation of the nonlinear system of latently infected CD4+ T cells along with the error-based mean fitness function of the system is as follows.

$$\begin{aligned}
\frac{d\tilde{X}}{dt}-\mu+d\tilde{X}+\alpha\tilde{X}\tilde{V}=0\;X(0)=I_1, \\
\frac{d\tilde{W}}{dt}+(q-1)\,\alpha\tilde{X}\tilde{V}+e\tilde{W}+\lambda\tilde{W}=0\;W(0)=I_2, \\
\frac{d\tilde{Y}}{dt}-\lambda\tilde{W}+\alpha\tilde{Y}-q\alpha\tilde{X}\tilde{V}=0\;Y(0)=I_3, \\
\frac{d\tilde{V}}{dt}+\tilde{V}-k\tilde{Y}=0\;V(0)=I_4,
\end{aligned} \tag{15}$$

D. CONSTRUCTION OF FITNESS FUNCTION

The fitness function of the proposed scheme is developed in an unsupervised manner by using the error function. The mathematical formulation of the fitness function with the constraints of the fitness function is presented in (16)-(21).

$$(\epsilon_X)2 = \frac{1}{N+1}\sum_{m=0}^{N}\left[\frac{d\tilde{X}}{dt} - \mu + d\tilde{X} + \alpha\tilde{X}\tilde{V} = 0\right]^2 \tag{16}$$

$$(\epsilon_W)2 = \frac{1}{N+1}\sum_{m=0}^{N} \times \left[\frac{d\tilde{W}}{dt} + (q-1)\,\alpha\tilde{X}\tilde{V} + e\tilde{W} + \lambda\tilde{W} = 0\right]^2 \tag{17}$$

$$(\epsilon_Y)2 = \frac{1}{N+1}\sum_{m=0}^{N}\left[\frac{d\tilde{Y}}{dt} - \lambda\tilde{W} + \alpha\tilde{Y} - q\alpha\tilde{X}\tilde{V} = 0\right]^2 \tag{18}$$

$$(\epsilon_V)2 = \frac{1}{N+1}\sum_{m=0}^{N}\left[\frac{d\tilde{V}}{dt} + \tilde{V} - k\tilde{Y} = 0\right]^2 \tag{19}$$

$$(\epsilon)2 = \frac{1}{4}\left[\left(\tilde{X}0 - I1\right)^2 + \left(\tilde{W}0 - I2\right)^2 + \left(\tilde{Y}0 - I3\right)^2 + \left(\tilde{V}0 - I4\right)^2\right] \tag{20}$$

$$\begin{aligned}\epsilon_{XWYV} = &\left[\left(\frac{1}{N+1}\sum_{m=0}^{N}\left[\frac{d\tilde{X}}{dt} - \mu + d\tilde{X} + \alpha\tilde{X}\tilde{V} = 0\right]^2\right.\right. \\ &+ \frac{1}{N+1}\sum_{m=0}^{N} \times \left[\frac{d\tilde{W}}{dt} + (q-1)\,\alpha\tilde{X}\tilde{V} + e\tilde{W} + \lambda\tilde{W} = 0\right]^2 \\ &+ \frac{1}{N+1}\sum_{m=0}^{N} \times \left[\frac{d\tilde{Y}}{dt} - \lambda\tilde{W} + \alpha\tilde{Y} - q\alpha\tilde{X}\tilde{V} = 0\right]^2 \\ &+ \frac{1}{N+1}\sum_{m=0}^{N}\left[\frac{d\tilde{V}}{dt} + \tilde{V} - k\tilde{Y} = 0\right]^2 \\ &\left.\left. + \frac{1}{4}\left[\left(\tilde{X}0 - I1\right)^2 + \left(\tilde{W}0 - I2\right)^2 + \left(\tilde{Y}0 - I3\right)^2 + \left(\tilde{V}0 - I4\right)^2\right]\right]\end{aligned} \tag{21}$$

E. OPTIMIZATION

PSO is a global optimizer algorithm that is based on the natural behavior of objects like birds flocking and the community-based social relation of humans.

The core concept of the PSO is the position and velocity of the particles like the weights of the neural network, birds in the flock in the individuals in the social community. For each iteration, the velocity of the particles is updated by using the position of the particle called pi and the position of the particles with each particle of the population called the pg. During the last few decades, the use of the PSO has been promising to solve optimization problems. PSO has been used as an optimization method in a variety of applications [53], [54], [55], [56].

PSO has many advantages over the other global optimization algorithms for instance, in contrast to the GA the PSO is less complex for function evaluation because the PSO does not use additional operations like a crossover, selection operator, etc.

Algorithm 1 Proposed Hybrid PSO-NMSM

Step 1: *Initialization of the Particles*

Create a primary swarm as a set of arbitrarily dispersed particles using constrained real values. These values should have better search space to be spared. A candidate solution has been assigned to each particle of the unknown parameters of the MHW-HIVFFANN-PSO-NMSM.

$P = [\alpha_1, \alpha_2, \alpha_3 \ldots \alpha_n, b_1, b_2, b_3 \ldots b_n, w_1, w_2, w_3 \ldots, w_n]$

Step 2: *Formulation of Fitness Evaluation Function and evaluation*

The fitness evaluation function has been formulated using Eq.16 and its fitness value is calculated for each particle while the velocity and position updating have been carried by the standard equations of the PSO algorithm available in the literature.

Step 3: *Termination criteria*

Terminate the execution of PSO if any one of the following conditions fulfills

- *Predefined fitness value achieved*
- *A maximum number of iterations are executed*
- *Tolcon* $= 10^{-12}$

If termination criteria meet then go to step 6 else continue.

Step 4: *Ranking*

Updated the global and local best particles of the swarm and ranked them according to the maximum fitness

Step 5: *Renewal of particle by updating the velocity and position*

Updated velocity and position of the particles using Eq.22. Repeat steps 2 to 5 until the total number of flights is completed

Step 6: *Refinement using the Nelder Mead Simplex Method*

Fine-tuning of the results obtained from the PSO is performed using the Nelder Mead Simplex, in this regard the best particles obtained for PSO are given to the local optimizer as a starting point.

Step 7: *Data storage for statistical analysis*

- *Store the weights of the best particle of the network*
- *Store the best fitness values*
- *Store the execution Time*

TABLE 1. Parameters setting for proposed PSO-NMSM.

PSO		Nadler Mead Simplex Method			
Parameters	Setting	Parameters	Setting		
Swarm size	100	Start point	The output of the PSO (Best Particles)		
Particle size	30		Minimum	Maximum	increment
Flights	1000	Reflection (α)	0.50	2.00	0.25
c1	(2.5–0.5)	Contraction (β)	0.25	0.75	0.25
c2	(0.5–2.5)	Expansion (γ)	1.50	3.00	0.25
Ω	0.9–0.4	Size of Simplex (A)	0.25	0.75	0.25
Vmax	0.2				
Population span	(−25, 25)				
Velocity span	(−2, 2)				

The major disadvantage of the SPO is it is stuck in global optima and unable to give the best local solution to the problem. To solve the constraint optimization problems, Nelder Mead's simplex algorithm is a local search optimization algorithm and was found to be promising in different applications. The working and application of the Nelder Mean Simplex Method minimization have been found in [57] and [58]. The major disadvantage of the NMSM is it struck in local optima and is unable to give the best global solution. The mutual strength of the PSO and NMSM algorithm is used to optimize the unknown design parameters of the proposed neural network to solve the coupled nonlinear HIV infection model of Latently Infected cells. The hybrid PSO-NMSM is presented in algorithm 1. The parameters used by hybrid PSO-NMSM are tabulated in Table 1.

For reliability, repeat steps 1 to 6 for a sufficiently large number of independent runs to get the results for a comprehensive statistical analysis.

F. PERFORMANCE INDICES

To check the reliability of the proposed scheme, the results have been analyzed by using different performance indicators, for instance, Absolute Error (AE), Global Mean Absolute Error (GMAE), Mean Squared Error (MSE), Global Mean Squared Error (GMSE), Mean Absolute Deviation in term of Absolute Error (MAD), and Global Mean Absolute Deviation (GMAD). The equation of the AE, MSE, GMSE, MAD, and GMAD is shown in (22)-(26).

$$E = \frac{\sum_{K=1}^{n} \left| Q0 - \tilde{Q}0 \right|}{K} \tag{22}$$

$$MSE = \sqrt{\frac{\sum_{K=1}^{n} \left| Q0 - \tilde{Q}0 \right|}{K}} \tag{23}$$

$$GMSE = \sum_{i=1}^{100} \left[\frac{\sum_{K=1}^{n} \left| Q0 - \tilde{Q}0 \right|}{K} \right] \tag{24}$$

$$MAD = \frac{\sum_{K=1}^{n} \left| Q0 - \tilde{Q}0 \right|}{K} \tag{25}$$

TABLE 2. Parameter setting for nonlinear system of latently infected CD4+ T cells [38].

Parameter	Value Case 1	Value Case 2
μ	0.4	0.5
λ	0.3	0.4
d	0.01	0.02
q	0.08	0.09
I_1	7	8
I_2	2	4
I_3	1	3
I_4	4	5
α	0.04	0.05
e	0.1	0.3
a	0.2	0.4
u	0.03	0.05
k	0.6	0.7

$$GMAD = \sum_{i=1}^{100} \left[\frac{\sum_{K=1}^{n} \left| Q0 - \tilde{Q}0 \right|}{K} \right] \tag{26}$$

where Q can be represented as X, W, Y, and V respectively. The study also investigated the MET to check the computational complexity of the proposed scheme over the existing, ANN-GASQP, ANN-PSO-SQP, PSO, and NAMS optimizer

III. SIMULATIONS AND RESULTS

This section discussed the solution of the nonlinear system of latently infected CD4+ T cells presented in (1). The performance of the proposed hybrid MHW-HIV FFADNN-PSO-NMSM is analyzed by using the comparative analysis of the results with the results presented in [38] and the solution of PSO-SQP. To validate the accuracy, precision, and reliability of the proposed scheme, an inclusive statistical analysis has also been performed in this section.

The reference solution of the nonlinear system of latently infected CD4+ T cells using (1) with parameter values presented in Table 2 for RK solver, ANN-based solution presented in [38], ANN-based PSO-SQP solver and proposed scheme are obtained for the input values with range 0-1 and step function of 0.1. The results of the proposed MHW-HIVFFADNN-PSO-NMSM are analyzed with RK based solver, ANN-based solver presented in [38], and ANN-PSO-SQP solver in terms of Absolute Error (AE).

To solve the nonlinear system presented in (1), the weights of the proposed MHW-ANN are optimized with PSO-NMSM. The best weights are gained with the 100 number of independent runs while using the 10 number of neurons. Figure 3 depicts the best weights gained by Particle Swarm Optimization (PSO), Nelder Mead Simplex Method

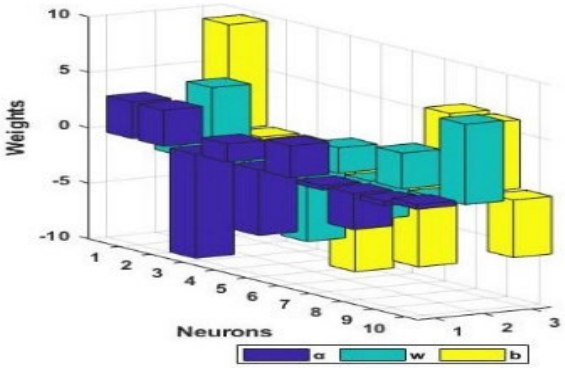

(a):

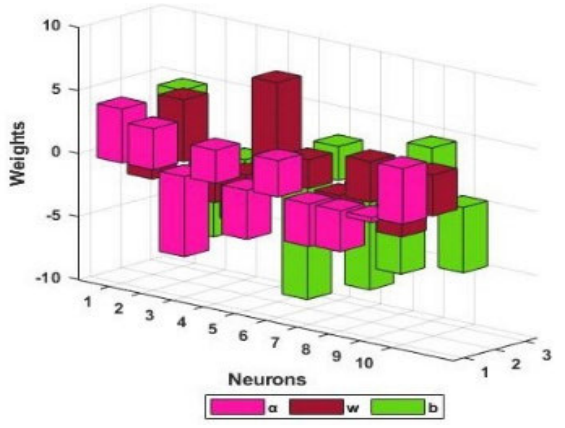

(b):

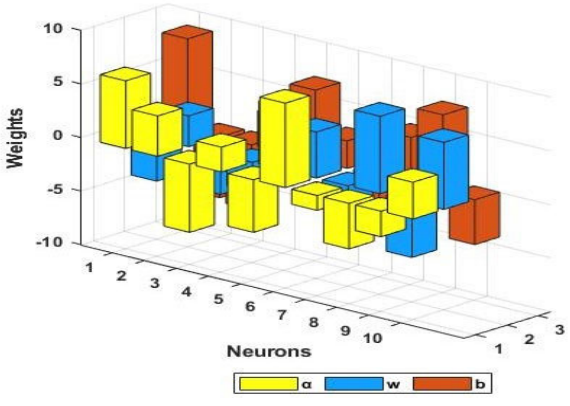

(c):

FIGURE 3. Best weights gained by (a) PSO, (b) Nelder mead simplex method and (c) Proposed PSO-NMSM.

(NMSM), and hybrid (PSO-NMSM). These weights are used to calculate the approximate solution of the system-based latently infected CD4+ T cells.

The obtained results of MSE for PSO, NMSM, and PSO-NMSM are plotted in Figure 4 while Figure 5 shows the best Mean Absolute Deviation (MAD) values in terms AE for PSO, NMSM, and PSO-NMSM. These values are obtained by Eq. (24) and Eq. (26). It is evident that the MSE values lies in the range of 6.50 E-07 to 8.30 E-04, 6.30 E-06 to 7.50 E-04 and 7.20 E-09 to 3.60 E-06 for PSO, NMSM and hybrid PSO-NMSM respectively. The values of MAD are in the range

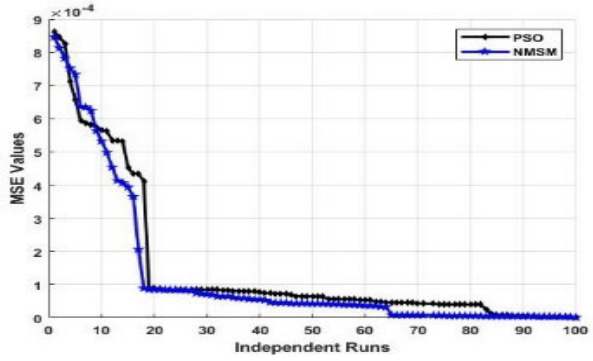

(a):

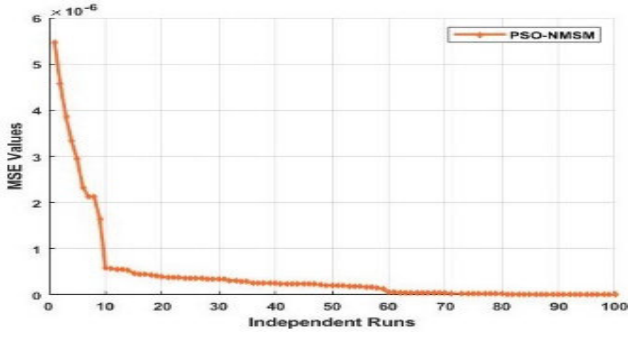

(b):

FIGURE 4. Mean square error values (a) PSO, NMSM (b) Proposed PSO-NMSM.

6.25 E-06 to 8.15 E-04, 9.50 E-06 to 6.30 E-04, 7.20 E-11 to 9.10 E-06.

To check the accuracy of the proposed scheme, the solution of the system presented in (1) having the classes X(t), W(t), Y(t), and V(t) for numerical solution and $\tilde{X}(t)$, $\tilde{W}(t)$, $\tilde{Y}(t)$ and $\tilde{V}(t)$ for ANN-based solutions is also presented. The system presented in (27) is used to approximate the solution of the nonlinear HIV infection model of Latently Infected CD4+ T cells. One can conclude that GA-SQP, PSO-SQP with log sigmoid, and the proposed MHW-HIVFFADNN-PSO-NMSM solved the system accurately. it has also been observed that the proposed MHW-PSO-NMSM outperforms in terms of Absolute Error (AE).

$$
\begin{aligned}
&\epsilon_{XWYV} \\
&= \left[\left(\frac{1}{11} \sum_{m=0}^{N} \left[\frac{d\tilde{X}}{dt} - (0.4) + d(0.01) + (0.04)\tilde{X}\tilde{V} \right]^2 \right. \right. \\
&\quad + \frac{1}{11} \sum_{m=0}^{N} \left[\frac{d\tilde{W}}{dt} + ((0.08) - 1)(0.04)\tilde{X}\tilde{V} + (0.1)\tilde{W} \right. \\
&\quad \left. \left. + (0.3)\tilde{W} \right]^2 \right. \\
&\quad + \frac{1}{11} \sum_{m=0}^{N} \left[\frac{d\tilde{Y}}{dt} - (0.3)\tilde{W} + (0.04)\tilde{Y} \right. \\
&\quad \left. \left. - (0.08)(0.04)\tilde{X}\tilde{V} \right]^2 + \frac{1}{11} \sum_{m=0}^{N}
\end{aligned}
$$

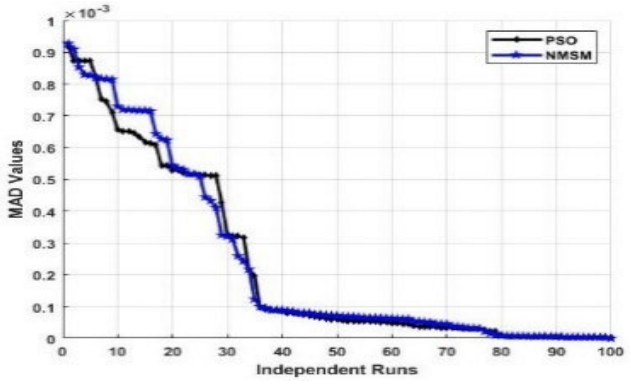

(a):

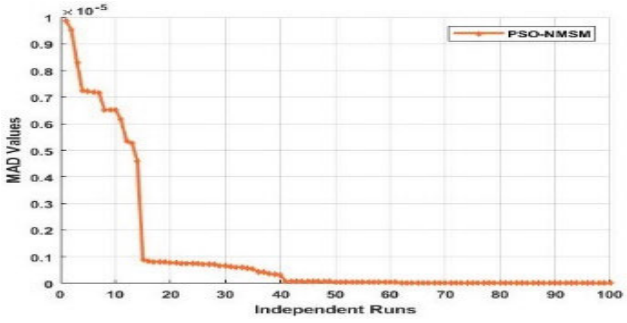

(b):

FIGURE 5. Mean average deviation values (a) PSO, NMSM (b) Proposed PSO-NMSM.

$$\times\left[\frac{d\tilde{V}}{dt}+\tilde{V}-(0.6)\tilde{Y}=0\right]^2 +\frac{1}{4}\left[\left(\tilde{X}0-7\right)^2+\left(\tilde{W}0-2\right)^2+\left(\tilde{Y}0-1\right)^2 +\left(\tilde{V}0-3\right)^2\right]\Big] \tag{27}$$

The solution of the nonlinear system, based on Latently Infected CD4+ T cells is plotted in Figure 6 while Figure 7 depicts the AE of numerical, ANN GA-SQP, ANN PSO-SQP, and proposed MHW-HIV FFADNN-PSO-NMSM solvers.

To validate the robustness of the proposed scheme, the solution of the non-linear system of Latently Infected CD4+ T cells is also evaluated through the different parameter values of the system. The system presented in (28) is used to evaluate the solution for the second case. The values for case 2 have been tabulated in Table 2. It is evident that the results are consistent and overlap with the analytical solution.

$$\epsilon_{XWYV} = \left[\left(\frac{1}{11}\sum_{m=0}^{N}\left[\frac{d\tilde{X}}{dt}-(0.5)+d(0.02)+(0.05)\tilde{X}\tilde{V}\right]^2 +\frac{1}{11}\sum_{m=0}^{N}\left[\frac{d\tilde{W}}{dt}+((0.09)-1)(0.05)\tilde{X}\tilde{V}\right]\right.\right.$$

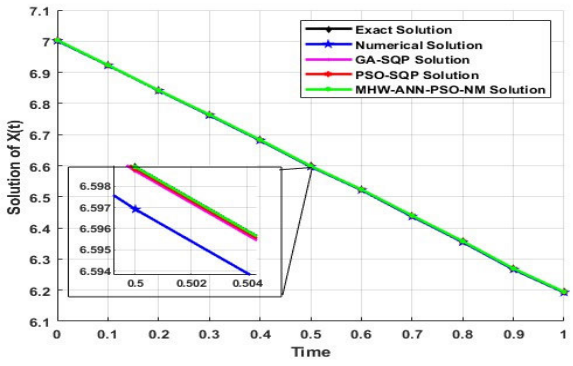

(a):

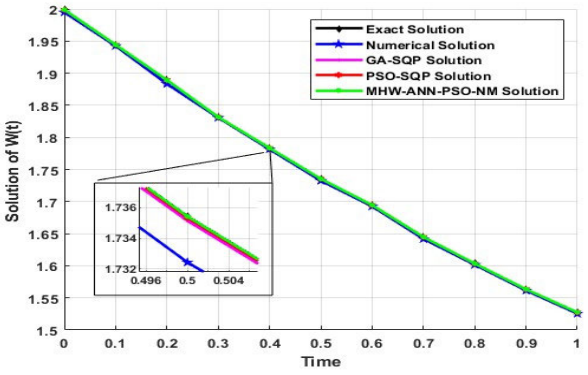

(b):

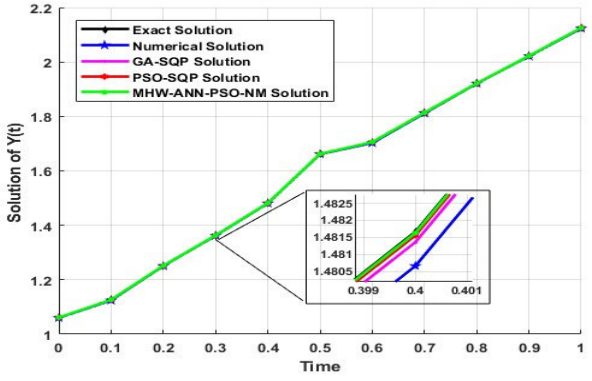

(c):

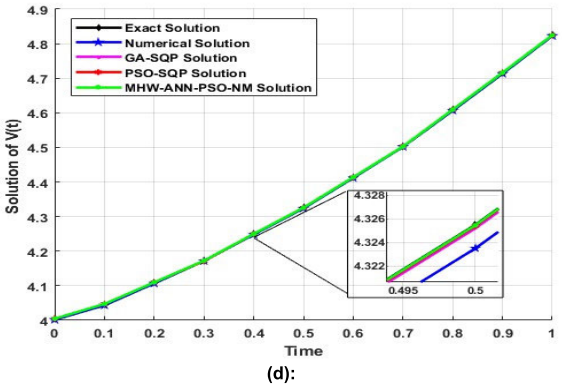

(d):

FIGURE 6. Solutions for analytical, numerical, GA-SQP, and Proposed PSO-NASM (a) $\tilde{X}(t)$, (b) $\tilde{W}(t)$, (c) $\tilde{Y}(t)$, (d) $\tilde{V}(t)$ for case 1.

$$+(0.3)\tilde{W}+(0.4)\tilde{W}\Big]^2+\frac{1}{11}\sum_{m=0}^{N}\left[\frac{d\tilde{Y}}{dt}-(0.4)\tilde{W}\right.$$
$$+(0.05)\tilde{Y}-(0.09)(0.05)\tilde{X}\tilde{V}\Big]^2+\frac{1}{11}\sum_{m=0}^{N}\left[\frac{d\tilde{V}}{dt}+\tilde{V}\right.$$
$$-(0.7)\tilde{Y}=0\Big]^2+\frac{1}{4}\left[\left(\tilde{X}0-8\right)^2+\left(\tilde{W}0-4\right)^2\right.$$
$$\left.+\left(\tilde{Y}0-3\right)^2+\left(\tilde{V}0-5\right)^2\right]\Big] \tag{28}$$

The solution for $\tilde{X}(t)$, $\tilde{W}(t)$, $\tilde{W}(t)$, and $\tilde{V}(t)$ along with the absolute error are shown in Figures 8 and Figure 9.

The AE for case 2 for the solution of the nonlinear coupled system of latently infected cells is shown in Figure 9.

It can be observed that the minimum AE values lie in the range E-04, E -05, and E -06 for numerical solvers, ANN GA-SQP, PSO-SQP, and proposed MHW-HIVFFADNN-PSO-NMSM for classes $\tilde{X}(t)$, $\tilde{W}(t)$, $\tilde{W}(t)$ and $\tilde{V}(t)$ respectively. The convergence analysis of the PSO, NMSM, GA-SQP, PSO-SQP, and the proposed PSO-NMSM has also been performed. Results for fitness values and MSE are presented in Table. 4. It is evident that the GA-SQP, PSO-SQP, and PSO-NMSM converged in all cases for the values 10^{-6}, $10^{-7,}$ and 10^{-8} for fitness values and 10^{-7}, $10^{-9,}$ and 10^{-11} for MSE values. However, the convergence of the proposed PSO-NMSM is much better than the GA-SQP and PSO-SQP due to the high computational complexity of the GA and SQP algorithms. PSO with the Nelder Mead Simplex method converged fast in all cases.

To validate the precision and accuracy of the proposed scheme, statistical investigation in terms of mean, median, and Standard deviation was also made. The results are tabulated in Table 3a, Table 3b, Table 3c, and Table 3d. Results show that the ANN-GA-SQP, PSO-SQP, and proposed MHW-HIVFFADNN-PSO-NMSM are consistent, precise, and accurate.

To confirm the global convergence and reliability of the proposed scheme, Global performance operator GMAD and GMSE for 100 independent runs are also examined. The values of the proposed MHW-HIV FFADNN-PSO-NMSM outperform the PSO and NMSM. The GMSE values are in the range 8.15E-09, 3.25E-10, 4.15E-09, and 3.15E-10 for $\tilde{X}(t)$, $\tilde{W}(t)$, $\tilde{Y}(t)$, and $\tilde{V}(t)$ classes respectively. Whereas the GMAD for the proposed scheme lies in the range 7.35E-09, 8.50E-10, 2.10E-10, and 7.10E-09.

IV. DISCUSSIONS

This section deals with a detailed discussion of the results carried out in the previous section. This discussion includes the Mean Absolute Error, computational time analysis, global mean Absolute error, and global mean Average deviation.

The accuracy of the proposed scheme along with the convergence analysis has been carried out by measuring the values of MAE and fitness values for the large number of independent runs. The convergence analysis has been verified through different convergence measures. For 100 runs the proposed schemes converge on $10^{-6,}10^{-7,}$ $10^{-8,}$ for fitness values and $10^{-7,}$ $10^{-9,}10^{-11}$ for the MSE values. The results of fitness values and the MAE are tabulated in Table 4. From

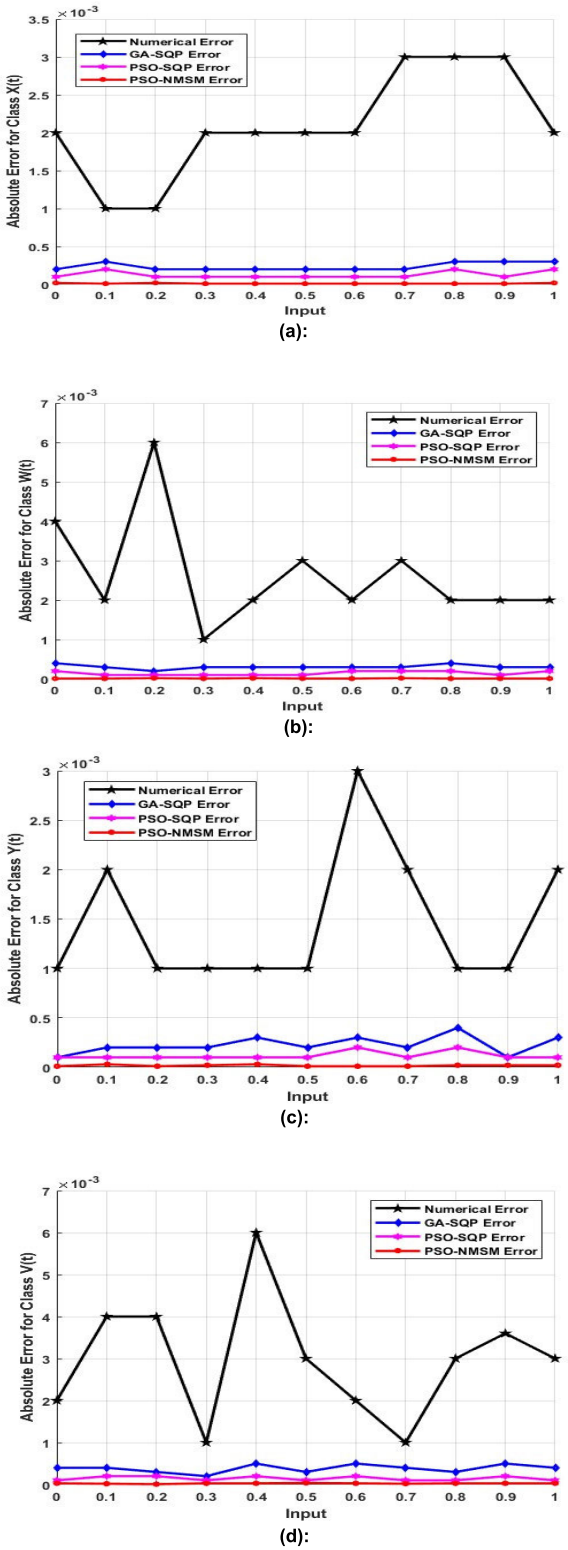

FIGURE 7. Absolute error (a) Numerical, (b) ANN-GA-SQP, and (c) PSO-NMSM.

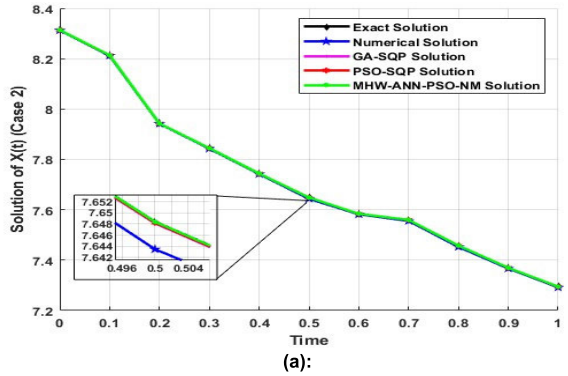

(a):

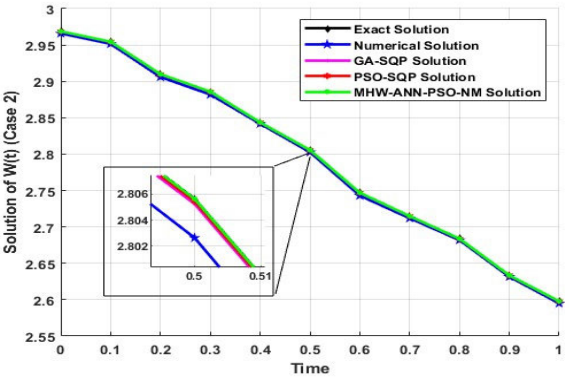

(b):

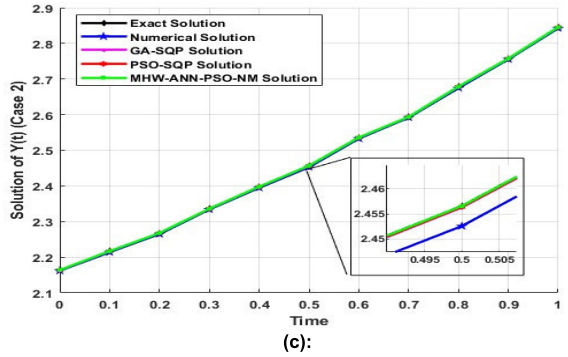

(c):

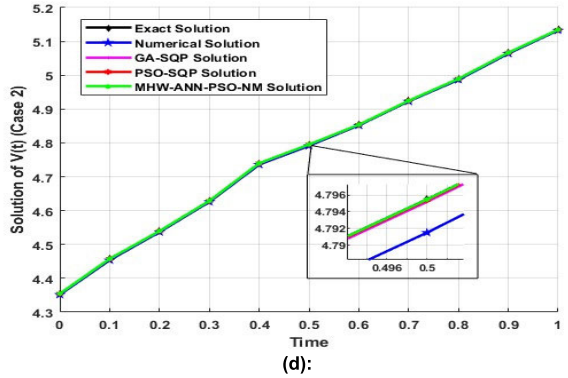

(d):

FIGURE 8. Solutions for analytical, numerical, GA-SQP, and Proposed PSO-NASM (a) $\tilde{X}(t)$, (b) $\tilde{W}(t)$, (c) $\tilde{Y}(t)$, (d) $\tilde{V}(t)$ for case 2.

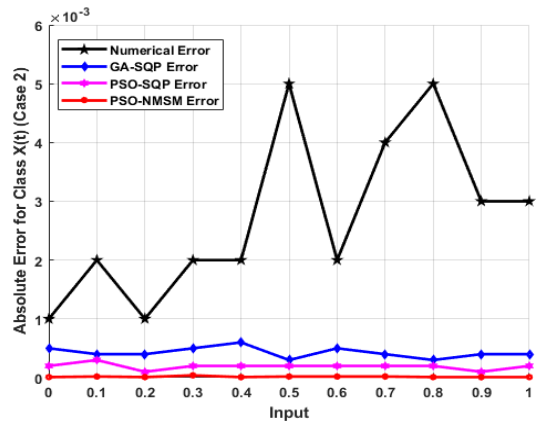

(a):

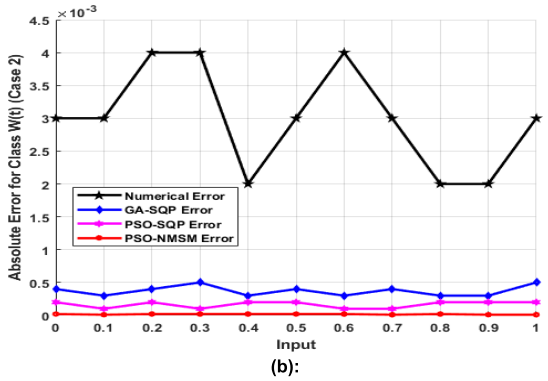

(b):

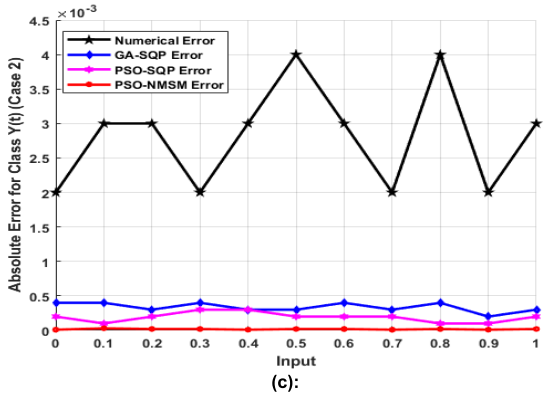

(c):

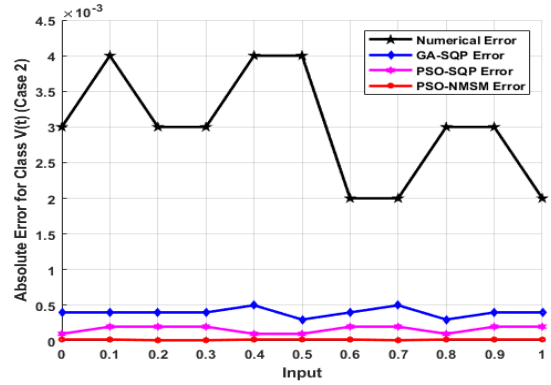

(d):

FIGURE 9. Absolute error (a) Numerical, (b) ANN-GA-SQP, and (c) PSO-NMSM for case 2.

TABLE 3. A) Statistical analysis of the proposed MHW-HIV FFADNN-PSO-NMSM for class $\tilde{X}(t)$, B) Statistical analysis of the proposed MHW-HIV FFADNN-PSO-NMSM for class $\tilde{W}(t)$, C) Statistical analysis of the proposed MHW-HIV FFADNN-PSO-NMSM for class $\tilde{Y}()$, D) Statistical analysis of the proposed MHW-HIV FFADNN-PSO-NMSM for class $\tilde{V}(t)$.

t	Min	Mean	Std
0	5.20E-11	6.75E-08	7.15E-06
0.1	7.23E-06	7.23E-10	3.75E-09
0.2	6.20E-07	8.60E-09	3.75E-08
0.3	7.30E-06	7.76E-08	8.26E-09
0.4	3.35E-07	9.58E-08	7.25E-08
0.5	3.20E-09	3.25E-09	7.22E-09
0.6	7.20E-06	3.15E-11	6.25E-08
0.7	4.58E-07	5.35E-07	8.25E-09
0.8	2.55E-11	8.55E-06	3.30E-09
0.9	8.25E-06	7.50E-09	3.20E-09
1	7.35E-07	3.40E-08	8.25E-08

(a)

t	Min	Mean	Std
0	6.25E-07	3.50E-11	3.10E-12
0.1	6.10E-11	7.50E-08	3.57E-08
0.2	5.25E-08	6.55E-09	3.55E-08
0.3	8.30E-10	2.70E-07	3.20E-09
0.4	7.25E-09	5.20E-08	5.65E-08
0.5	3.75E-08	3.20E-08	9.15E-09
0.6	3.15E-08	7.25E-09	8.25E-09
0.7	7.36E-09	2.25E-10	3.50E-08
0.8	2.55E-11	6.50E-08	5.65E-08
0.9	8.70E-09	6.20E-09	4.10E-09
1	7.50E-10	7.25E-08	3.80E-09

(b)

t	Min	Mean	Std
0	7.25E-08	7.85E-11	2.30E-09
0.1	8.20E-11	3.80E-08	5.65E-08
0.2	4.35E-08	6.20E-07	4.35E-09
0.3	2.25E-07	4.65E-08	3.20E-12
0.4	6.25E-07	2.15E-08	6.35E-06
0.5	8.25E-08	8.75E-07	8.25E-09
0.6	7.20E-09	3.15E-08	3.50E-07
0.7	6.50E-10	7.85E-09	7.30E-12
0.8	3.50E-09	5.20E-09	2.50E-08
0.9	3.85E-09	6.70E-07	7.15E-07
1	2.05E-09	8.12E-07	4.70E-07

(c)

t	Min	Mean	Std
0	3.15E-08	3.80E-09	5.20E-09
0.1	2.10E-07	5.20E-08	6.65E-08
0.2	3.25E-10	8.20E-07	8.25E-09
0.3	8.50E-07	3.25E-11	7.12E-12
0.4	3.35E-11	7.35E-08	3.25E-08
0.5	2.25E-08	5.75E-07	2.35E-09
0.6	9.10E-09	4.55E-09	7.20E-09
0.7	7.25E-10	9.25E-09	3.20E-12
0.8	6.30E-09	8.10E-09	2.50E-09
0.9	4.50E-09	3.20E-07	3.15E-07
1	2.05E-09	8.12E-07	4.70E-07

(d)

Table 4 it can be observed that the GA-SQP, PSO-SQP, and the proposed PSO-NMSM have a maximum convergence rate

TABLE 4. Convergence analysis with fitness values and MSE values with different levels.

	Method	% Runs with Fitness Value			% Runs with MSE		
		10^{-6}	10^{-7}	10^{-8}	10^{-7}	10^{-9}	10^{-11}
$\tilde{X}(t)$	PSO	95	96	94	97	95	98
	GA-SQP	**100**	**100**	**100**	**100**	**100**	**100**
	PSO-SQP	**100**	**100**	**100**	**100**	**100**	**100**
	PSO-NMSM	**100**	**100**	**100**	**100**	**100**	**100**
$\tilde{W}(t)$	PSO	95	97	96	97	93	95
	GA-SQP	**100**	**100**	**100**	**100**	**100**	**100**
	PSO-SQP	**100**	**100**	**100**	**100**	**100**	**100**
	PSO-NMSM	**100**	**100**	**100**	**100**	**100**	**100**
$\tilde{Y}(t)$	PSO	97	94	97	96	97	96
	GA-SQP	**100**	**100**	**100**	**100**	**100**	**100**
	PSO-SQP	**100**	**100**	**100**	**100**	**100**	**100**
	PSO-NMSM	**100**	**100**	**100**	**100**	**100**	**100**
$\tilde{V}(t)$	PSO	95	97	97	96	97	96
	GA-SQP	**100**	**100**	**100**	**100**	**100**	**100**
	PSO-SQP	**100**	**100**	**100**	**100**	**100**	**100**
	PSO-NMSM	**100**	**100**	**100**	**100**	**100**	**100**

for the conditions given. The proposed scheme converges with all classes and gives the most accurate solution.

The fitness functions ϵ_{XWYV} given in (17)-(21) are also examined for the 100 number of independent runs. By using the meeting conditions $10^{-7,}$ $10^{-9,}10^{-11}$ the results are tabulated in Table 4. It can be seen that the proposed hybrid PSO-NMSM scheme is consistent and converges in all classes to solve the nonlinear system of latently infected cells of CD4+ T, while the low convergence rate has been observed for PSO and NMSM and is unable to meet the required fitness.

The global statistical indicators, for instance, GMSE, and GMAD have also been examined through the 100 independent runs. The obtained results of GMSE and GMAD along with the STD are tabulated in Table 5. It is found that the values of the proposed MHW-HIV FFADNN optimized with the hybrid PSO-NMSM are best to obtain the solution and results are stable for a large number of runs. The Results of the proposed schemes are very close to the reference and the numerical solution with 6 decimal points. it is evident of the good agreement of the proposed scheme.

The computational complexity of the proposed (MHW-HIV FFADNN-PSO-NMSM) scheme has been analyzed through the average execution time. The complexity of the algorithm has been calculated for 100 liberated runs of the proposed scheme for $\tilde{X}(t)$, $\tilde{W}(t)$, $\tilde{Y}(t)$, and $\tilde{V}(t)$ classes respectively. The results are evidence that the computational

TABLE 5. Comparison through Global Performance Indicators GMSE and GMAD.

Equations	Method	GMSE		GMAD	
		Values	STD	Values	STD
$\tilde{X}(t)$	PSO	3.30E-05	7.55E-05	9.25E-04	3.25E-06
	NMSM	2.25E-04	6.25E-04	3.20E-05	8.15E-05
	GA-SQP	**8.25E-08**	**3.25E-07**	**6.25E-09**	**7.15E-09**
	PSO-SQP	**3.35E-08**	**9.40E-07**	**6.50E-09**	**8.25E-09**
	PSO-NMSM	**8.15E-09**	**5.33E-07**	**7.35E-09**	**5.20E-09**
$\tilde{W}(t)$	PSO	8.25E-05	8.35E-05	3.35E-06	9.20E-06
	NMSM	3.50E-03	2.55E-03	2.55E-04	6.10E-04
	GA-SQP	**9.72E-08**	**3.35E-08**	**7.50E-09**	**3.75E-09**
	PSO-SQP	**5.20E-08**	**8.60E-08**	**3.30E-09**	**9.15E-09**
	PSO-NMSM	**3.25E-10**	**7.15E-08**	**8.50E-10**	**6.55E-09**
$\tilde{Y}(t)$	PSO	2.25E-05	7.20E-05	3.20E-06	6.15E-06
	NMSM	5.75E-03	8.15E-03	2.50E-04	8.35E-04
	GA-SQP	**8.25E-08**	**3.25E-08**	**3.75E-09**	**7.25E-09**
	PSO-SQP	**4.15E-08**	**6.50E-08**	**7.35E-09**	**8.10E-09**
	PSO-NMSM	**4.15E-09**	**2.75E-08**	**2.10E-10**	**5.15E-09**
$\tilde{V}(t)$	PSO	7.25E-05	6.25E-05	9.10E-06	3.25E-06
	NMSM	3.15E-03	7.15E-03	6.20E-04	2.35E-04
	GA-SQP	**8.15E-08**	**3.35E-08**	**7.15E-09**	**7.15E-09**
	PSO-SQP	**5.50E-08**	**7.20E-08**	**4.10E-09**	**6.25E-09**
	PSO-NMSM	**3.15E-10**	**2.75E-08**	**7.10E-09**	**5.15E-09**

TABLE 6. Computational complexity of the PSO, NMSM, ANN-GA-SQP, and MHW-HIV FFADNN-PSO-NMSM.

Techniques	PSO	NMSM	GA-SQP	PSO-SQP	**PSO-NMSM**
MET (Minutes)	4.25	5.15	35.27	35.58	**20.20**

complexity of the proposed MHW-HIV FFADNN-PSO-NMSM is greater than the PSO and NMSM However, the proposed scheme has less computational complexity than the ANN-GA-SQP and PSO-SQP. The proposed scheme outperforms the ANN-GA-SQP and ANN PSO-SQP regarding computational complexity. The values for MET in minutes are tabulated in Table 6. The computations are carried out on HP Folio 9480 m, with an Intel (R) processor with RAM 8 GB, an I7 processor, an SSD drive, and MATLAB version 2020a.

V. CONCLUSION

This work presented a consistent, precise, and accurate ANN-based neuroheuristic method optimized with PSO, NMSM, and hybrid PSO-NMSM to solve the nonlinear system of latently infected CD4+ T cells. The weights of the proposed ANN-based solvers have been optimized with PSO and NMSM in a hybrid manner. Comparison of the proposed MHW-HIVFFADNN-PSO-NMSM with the analytical solution, numerical solution of the ANN-GA-SQP solution, ANN-PSO-SQP solution, and proposed solutions shows that the proposed scheme solves the system accurately and effectively for all classes, the results of the proposed scheme in terms of absolute error are E-06 for both cases which are better than the numerical solver which has absolute error E -04 and the ANN-based solver with absolute error E-06. The accuracy, convergence, and reliability of the proposed scheme were validated through a large number of independent runs. A comprehensive statistical analysis has also been performed. it is evident that the proposed scheme gives consistent convergence, and constant results for all cases of the nonlinear system of latently infected cells of the HIV model. The Global Mean Square Error (GMSE) of the proposed scheme is 8.15E-09 while the GMSE of the ANN solver based on GA-SQP, PSO-SQP and the PSO are 8.25E-08 and 2.25E-04 for class $\tilde{X}(t)$ while 3.25E-10, 9.72E-08, 8.25E-05, 4.15E-09, 8.25E-08, 2.25E-05, 3.15E-10, 8.15E-08, 7.25E-05 for $\tilde{W}(t)$, $\tilde{Y}(t)$, and $\tilde{V}(t)$ respectively. The computational complexity of the proposed scheme is 20.20 minutes which is high as compared to the PSO with an execution time of 4.25 minutes and NMSM with 5.15 minutes however, shows less complexity as compared with the ANN-GA-SQP and PSO-SQP whose execution time was 35.24 and 35.58 minutes. This is due to the hybrid nature of the proposed scheme. Nevertheless, the performance of the proposed scheme is better than the PSO and NMSM.

In the future different alternative schemes, for instance, ASA, ACO, GA along NMSM shall investigated. Furthermore, it will be interesting to use the proposed scheme to solve the non-linear system related to computer viruses, COVID-19, Dengue Fever, and other physical systems.

REFERENCES

[1] A. S. Perelson, D. E. Kirschner, and R. De Boer, "Dynamics of HIV infection of CD4+ T cells," *Math. Biosciences*, vol. 114, no. 1, pp. 81–125, Mar. 1993.

[2] N. Ali and G. Zaman, "Asymptotic behavior of HIV-1 epidemic model with infinite distributed intracellular delays," *SpringerPlus*, vol. 5, no. 1, pp. 1–13, Dec. 2016.

[3] I. E. Lagaris, A. Likas, and D. I. Fotiadis, "Artificial neural networks for solving ordinary and partial differential equations," *IEEE Trans. Neural Netw.*, vol. 9, no. 5, pp. 987–1000, Jun. 1998.

[4] N. Yadav, A. Yadav, and M. Kumar, *An Introduction to Neural Network Methods for Differential Equations*. Cham, Switzerland: Springer, 2015.

[5] A. Amirkhani, A. Khosravian, M. Masih-Tehrani, and H. Kashiani, "Robust semantic segmentation with multi-teacher knowledge distillation," *IEEE Access*, vol. 9, pp. 119049–119066, 2021.

[6] H. Nasiriyan-Rad, A. Amirkhani, A. Naimi, and K. Mohammadi, "Learning fuzzy cognitive map with PSO algorithm for grading celiac disease," in *Proc. 23rd Iranian Conf. Biomed. Eng. 1st Int. Iranian Conf. Biomed. Eng.*, Nov. 2016, pp. 341–346.

[7] H. Zhou, Y. Li, Q. Zhang, H. Xu, and Y. Su, "Soft-sensing of effluent total phosphorus using adaptive recurrent fuzzy neural network with gustafson-kessel clustering," *Expert Syst. Appl.*, vol. 203, Oct. 2022, Art. no. 117589.

[8] H. Zhou, Y. Zhang, W. Duan, and H. Zhao, "Nonlinear systems modelling based on self-organizing fuzzy neural network with hierarchical pruning scheme," *Appl. Soft Comput.*, vol. 95, Oct. 2020, Art. no. 106516.

[9] L. Yan, Z. Sabir, E. Ilhan, M. Asif Zahoor Raja, W. Gao, and H. Mehmet Baskonus, "Design of a computational heuristic to solve the nonlinear lienard differential model," *Comput. Model. Eng. Sci.*, vol. 136, pp. 201–221, Jul. 2023.

[10] M. Umar, Z. Sabir, M. A. Z. Raja, F. Amin, T. Saeed, and Y. G. Sanchez, "Design of intelligent computing solver with Morlet wavelet neural networks for nonlinear predator–prey model," *Appl. Soft Comput.*, vol. 134, Feb. 2023, Art. no. 109975.

[11] Z. Sabir, M. A. Z. Raja, M. R. Ali, and R. Sadat, "An advance computational intelligent approach to solve the third kind of nonlinear pantograph Lane–Emden differential system," *Evolving Syst.*, vol. 1, pp. 1–20, Oct. 2022.

[12] W. Adel, Z. Sabir, H. Rezazadeh, and A. Aldurayhim, "Application of a novel collocation approach for simulating a class of nonlinear third-order Lane–Emden model," *Math. Problems Eng.*, vol. 2022, pp. 1–16, Jun. 2022.

[13] M. A. Z. Raja, J. A. Khan, and T. Haroon, "Stochastic numerical treatment for thin film flow of third grade fluid using unsupervised neural networks," *J. Taiwan Inst. Chem. Engineers*, vol. 48, pp. 26–39, Mar. 2015.

[14] T. Botmart, Z. Sabir, M. A. Z. Raja, W. Weera, R. Sadat, and M. R. Ali, "Stochastic procedures to solve the nonlinear mass and heat transfer model of Williamson nanofluid past over a stretching sheet," *Ann. Nucl. Energy*, vol. 181, Feb. 2023, Art. no. 109564.

[15] F. A. Chaudhry, M. Amin, M. Iqbal, R. D. Khan, and J. A. Khan, "A novel chaotic differential evolution hybridized with quadratic programming for short-term hydrothermal coordination," *Neural Comput. Appl.*, vol. 30, no. 11, pp. 3533–3544, Dec. 2018.

[16] A. J. Joshy, R. Dunn, M. Sperry, V. E. Gandarillas, and J. T. Hwang, "An SQP algorithm based on a hybrid architecture for accelerating optimization of large-scale systems," in *Proc. AIAA Aviation Forum*, Jun. 2023, pp. 42–63.

[17] J. A. Khan, M. A. Z. Raja, M. M. Rashidi, M. I. Syam, and A. M. Wazwaz, "Nature-inspired computing approach for solving non-linear singular Emden–Fowler problem arising in electromagnetic theory," *Connection Sci.*, vol. 27, no. 4, pp. 377–396, Oct. 2015.

[18] Q. Nguyen, M. Onur, and F. O. Alpak, "Nonlinearly constrained life-cycle production optimization using sequential quadratic programming (SQP) with stochastic simplex approximated gradients (StoSAG)," in *Proc. SPE Reservoir Simul. Conf.*, Mar. 2023, pp. 1–28.

[19] M. A. Z. Raja, J. A. Khan, A. Zameer, N. A. Khan, and M. A. Manzar, "Numerical treatment of nonlinear singular flierl–petviashivili systems using neural networks models," *Neural Comput. Appl.*, vol. 31, no. 7, pp. 2371–2394, Jul. 2019.

[20] M. A. Z. Raja, J. A. Khan, N. I. Chaudhary, and E. Shivanian, "Reliable numerical treatment of nonlinear singular flierl–petviashivili equations for unbounded domain using ANN, GAs, and SQP," *Appl. Soft Comput.*, vol. 38, pp. 617–636, Jan. 2016.

[21] M. A. Z. Raja, M. Umar, Z. Sabir, J. A. Khan, and D. Baleanu, "A new stochastic computing paradigm for the dynamics of nonlinear singular heat conduction model of the human head," *Eur. Phys. J. Plus*, vol. 133, no. 9, pp. 1–21, Sep. 2018.

[22] Z. Sabir, D. Baleanu, M. R. Ali, and R. Sadat, "A novel computing stochastic algorithm to solve the nonlinear singular periodic boundary value problems," *Int. J. Comput. Math.*, vol. 99, no. 10, pp. 2091–2104, Oct. 2022.

[23] Z. Sabir, T. Botmart, M. A. Z. Raja, and W. Weera, "An advanced computing scheme for the numerical investigations of an infection-based fractional-order nonlinear prey-predator system," *PLoS One*, vol. 17, no. 3, 2022, Art. no. e026506.

[24] Z. Sabir, M. A. Z. Raja, A. S. Alnahdi, M. B. Jeelani, and M. A. Abdelkawy, "Numerical investigations of the nonlinear smoke model using the gudermannian neural networks," *Math. Biosciences Eng.*, vol. 19, no. 1, pp. 351–370, 2022.

[25] Z. Sabir, M. A. Z. Raja, S. R. Mahmoud, M. Balubaid, A. Algarni, A. H. Alghtani, A. A. Aly, and D.-N. Le, "A novel design of Morlet wavelet to solve the dynamics of nervous stomach nonlinear model," *Int. J. Comput. Intell. Syst.*, vol. 15, no. 1, p. 4, Jan. 2022.

[26] Z. Sabir, M. A. Z. Raja, M. Shoaib, R. Sadat, and M. R. Ali, "A novel design of a sixth-order nonlinear modeling for solving engineering phenomena based on neuro intelligence algorithm," *Eng. Comput.*, vol. 39, no. 3, pp. 1807–1822, Jun. 2023.

[27] Z. Sabir, T. Saeed, J. L. G. Guirao, J. M. Sánchez, and A. Valverde, "A swarming Meyer wavelet computing approach to solve the transport system of goods," *Axioms*, vol. 12, no. 5, p. 456, May 2023.

[28] S. Suantai, Z. Sabir, M. A. Z. Raja, and W. Cholamjiak, "Swarming computational procedures for the coronavirus-based mathematical SEIR-NDC model," *J. Math.*, vol. 2022, pp. 1–18, Oct. 2022.

[29] Z. Sabir, M. A. Z. Raja, S. E. Alhazmi, M. Gupta, A. Arbi, and I. A. Baba, "Applications of artificial neural network to solve the nonlinear COVID-19 mathematical model based on the dynamics of SIQ," *J. Taibah Univ. Sci.*, vol. 16, no. 1, pp. 874–884, Dec. 2022.

[30] M. Umar, Z. Sabir, M. A. Z. Raja, M. Shoaib, M. Gupta, and Y. G. Sánchez, "A stochastic intelligent computing with neuro-evolution heuristics for nonlinear SITR system of novel COVID-19 dynamics," *Symmetry*, vol. 12, no. 10, p. 1628, Oct. 2020.

[31] M. Umar, Z. Sabir, M. A. Z. Raja, S. Javeed, H. Ahmad, S. K. Elagen, and A. Khames, "Numerical investigations through ANNs for solving COVID-19 model," *Int. J. Environ. Res. Public Health*, vol. 18, no. 22, p. 12192, Nov. 2021.

[32] M. Umar, Z. Sabir, M. A. Z. Raja, F. Amin, T. Saeed, and Y. Guerrero-Sanchez, "Integrated neuro-swarm heuristic with interior-point for nonlinear SITR model for dynamics of novel COVID-19," *Alexandria Eng. J.*, vol. 60, no. 3, pp. 2811–2824, Jun. 2021.

[33] Y. G. Sánchez, Z. Sabir, and J. L. G. Guirao, "Design of a nonlinear Sierpinski iterated function system (IFS) fractal model based on the dynamics of a novel coronavirus (COVID-19)," *Fractals*, vol. 28, no. 8, Dec. 2020, Art. no. 2040026.

[34] Z. Sabir, M. A. Z. Raja, H. M. Baskonus, and A. Ciancio, "Numerical performance using the neural networks to solve the nonlinear biological quarantined based COVID-19 model," *Atti della Accademia Peloritana Dei Pericolanti-Classe Di Scienze Fisiche, Matematiche E Naturali*, vol. 1, no. 1, p. 10, 2023.

[35] A. Elsonbaty, Z. Sabir, R. Ramaswamy, and W. Adel, "Dynamical analysis of a novel discrete fractional SiTrS model for COVID-19," *Fractals*, vol. 29, no. 8, Dec. 2021, Art. no. 2140035.

[36] T. Botmart, Z. Sabir, S. Javeed, R. A. Sandoval Nuñez, W. Weera, M. R. Ali, and R. Sadat, "Artificial neural network-based heuristic to solve COVID-19 model including government strategies and individual responses," *Informat. Med. Unlocked*, vol. 32, Jun. 2022, Art. no. 101028.

[37] A. N. Akkilic, Z. Sabir, M. A. Z. Raja, and H. Bulut, "Numerical treatment on the new fractional-order SIDARTHE COVID-19 pandemic differential model via neural networks," *Eur. Phys. J. Plus*, vol. 137, no. 3, p. 334, Mar. 2022.

[38] M. Umar, Z. Sabir, M. A. Z. Raja, H. M. Baskonus, S.-W. Yao, and E. Ilhan, "A novel study of Morlet neural networks to solve the nonlinear HIV infection system of latently infected cells," *Results Phys.*, vol. 25, Jun. 2021, Art. no. 104235.

[39] Z. Sabir, M. Umar, M. A. Z. Raja, H. M. Baskonus, and W. Gao, "Designing of Morlet wavelet as a neural network for a novel prevention category in the HIV system," *Int. J. Biomathematics*, vol. 15, no. 4, May 2022, Art. no. 2250012.

[40] Z. Sabir, M. Umar, M. Asif Zahoor Raja, and D. Baleanu, "Numerical solutions of a novel designed prevention class in the HIV nonlinear model," *Comput. Model. Eng. Sci.*, vol. 129, no. 1, pp. 227–251, 2021.

[41] M. Umar, Z. Sabir, M. A. Zahoor Raja, K. S. Al-Basyouni, S. R. Mahmoud, and Y. G. Sánchez, "An advance computing numerical heuristic of nonlinear SIR dengue fever system using the Morlet wavelet kernel," *J. Healthcare Eng.*, vol. 2022, pp. 1–14, Jan. 2022.

[42] M. Umar, Z. Sabir, M. A. Z. Raja, and Y. G. Sánchez, "A stochastic numerical computing heuristic of SIR nonlinear model based on dengue fever," *Results Phys.*, vol. 19, Dec. 2020, Art. no. 103585.

[43] M. Umar, M. A. Z. Raja, Z. Sabir, and Q. Al-Mdallal, "A computational framework to solve the nonlinear dengue fever SIR system," *Comput. Methods Biomechanics Biomed. Eng.*, vol. 25, no. 16, pp. 1821–1834, Dec. 2022.

[44] Z. Sabir, M. A. Z. Raja, S. Javeed, and Y. Guerrero-Sánchez, "Numerical investigations of a fractional nonlinear dengue model using artificial neural networks," *Fractals*, vol. 30, no. 10, pp. 1–12, Dec. 2022.

[45] P. Junsawang, S. Zuhra, Z. Sabir, M. A. Z. Raja, M. Shoaib, T. Botmart, and W. Weera, "Numerical simulations of vaccination and Wolbachia on dengue transmission dynamics in the nonlinear model," *IEEE Access*, vol. 10, pp. 31116–31144, 2022.

[46] M. Umar, Z. Sabir, M. A. Z. Raja, H. M. Baskonus, M. R. Ali, and N. A. Shah, "Heuristic computing with sequential quadratic programming for solving a nonlinear hepatitis B virus model," *Math. Comput. Simul.*, vol. 212, pp. 234–248, Oct. 2023.

[47] Z. Sabir, S. Ben Said, and Q. Al-Mdallal, "A fractional order numerical study for the influenza disease mathematical model," *Alexandria Eng. J.*, vol. 65, pp. 615–626, Feb. 2023.

[48] Z. Sabir, T. Botmart, M. A. Z. Raja, W. Weera, R. Sadat, M. R. Ali, A. A. Alsulami, and A. Alghamdi, "Artificial neural network scheme to solve the nonlinear influenza disease model," *Biomed. Signal Process. Control*, vol. 75, May 2022, Art. no. 103594.

[49] S. Noinang, Z. Sabir, G. Cieza Altamirano, M. A. Z. Raja, M. J. Sachez-Chero, M.-V. Seminario-Morales, W. Weera, and T. Botmart, "Swarming computational techniques for the influenza disease system," *Comput., Mater. Continua*, vol. 73, no. 3, pp. 4851–4868, 2022.

[50] S. Noinang, Z. Sabir, M. Asif Zahoor Raja, S. Salahshour, W. Weera, and T. Botmart, "Numerical procedure for fractional HBV infection with impact of antibody immune," *Comput., Mater. Continua*, vol. 74, no. 2, pp. 2575–2588, 2023.

[51] Z. Sabir, D. Baleanu, M. A. Z. Raja, A. S. Alshomrani, and E. Hincal, "Computational performances of Morlet wavelet neural network for solving a nonlinear dynamic based on the mathematical model of the affection of Layla and Majnun," *Fractals*, vol. 31, no. 2, Jan. 2023, Art. no. 2340016.
[52] Z. Masood, K. Majeed, R. Samar, and M. A. Z. Raja, "Design of Mexican hat wavelet neural networks for solving bratu type nonlinear systems," *Neurocomputing*, vol. 221, pp. 1–14, Jan. 2017.
[53] A. G. Gad, "Particle swarm optimization algorithm and its applications: A systematic review," *Arch. Comput. Methods Eng.*, vol. 29, no. 5, pp. 2531–2561, Aug. 2022.
[54] M. Jain, V. Saihjpal, N. Singh, and S. B. Singh, "An overview of variants and advancements of PSO algorithm," *Appl. Sci.*, vol. 12, no. 17, p. 8392, Aug. 2022.
[55] E. García-Gonzalo and J. L. Fernández-Martínez, "A brief historical review of particle swarm optimization (PSO)," *J. Bioinf. Intell. Control*, vol. 1, no. 1, pp. 3–16, Jun. 2012.
[56] S. G. Andrab, A. Hekmat, and Z. B. Yusop, "A review: Evolutionary computations (GA and PSO) in geotechnical engineering," *Comput. Water, Energy, Environ. Eng.*, vol. 6, no. 2, pp. 154–179, 2017.
[57] N. Pham, "Improved Nelder Mead's simplex method and applications," 2012.
[58] D. M. Olsson and L. S. Nelson, "The Nelder-Mead simplex procedure for function minimization," *Technometrics*, vol. 17, no. 1, p. 45, Feb. 1975.

FARHAD MUHAMMAD RIAZ is currently pursuing the Ph.D. degree in computer science with HITEC University, Taxila, Pakistan. He is also a Lecturer in computer science with the National University of Modern Languages, Islamabad. His research interests include mathematical modeling, neural network modeling, cognitive computing, ANN-based numerical approximation, and deep learning.

SHAFIQ AHMAD received the Ph.D. degree from RMIT University, Melbourne, Australia. He is currently an Associate Professor with the Industrial Engineering Department, College of Engineering, King Saud University, Riyadh, Saudi Arabia. He has more than two decades of working experience both in industry and academia in Australia, Europe, and Asia. He has published a research book and several research articles in international journals and refereed conferences. His research interests include smart manufacturing, the IIoT, data analytics, multivariate statistical quality control, process monitoring and performance analysis, operations research models, and bibliometric network analysis. He is also a certified practitioner in the Six Sigma business improvement model.

JUNIAD ALI KHAN received the Ph.D. degree in electronic engineering majoring in modeling of neural networks for non-linear systems from International Islamic University, Islamabad, in 2011. Currently, he is the Dean of the Faculty of Sciences and the Chair of the Department of Computer Science, HITEC University, Taxila, Pakistan. He has published more than 70 articles in various reputed relevant journals. His research interests include non-linear system modeling, cognitive computation, deep neural networks, and fuzzy systems. His recent projects involve applications of fuzzy DNN in earth observation and seismic analysis.

SAUD ALTAF received the master's degree in computer science from Iqra University, Islamabad, Pakistan, in 2007, and the Ph.D. degree in computer science from Auckland University of Technology (AUT), New Zealand, in 2015. He is currently a Professor with National Skills University, Islamabad. He is the author of a number of research publications in international impact factor journals or conference proceedings. His research interests include wireless sensor networks, biomedical signal and image processing, security of cyber-physical systems (CPS), gesture recognition, through-the-wall radar imaging and sensing, visible light communication, the Internet of Things (IoT), artificial intelligence, and data mining.

ZIA UR REHMAN received the master's degree in computer science from Muhammad Ali Jinnah University, Islamabad, Pakistan, in 2008, and the Ph.D. degree from the University Institute of Information Technology (UIIT), Pir Mehr Ali Shah Arid Agriculture University (PMAS—AAR), Rawalpindi, Pakistan, in 2023. He is currently an Assistant Professor with the Department of Computer Science, National University of Modern Languages (NUML). His major research interests include security issues in health monitoring aspects of cyber-physical systems (CPS), AI, the Internet of Things (IoT), and wireless sensor networks.

SHUAIB KARIM MEMON received the Ph.D. degree in computer science from Auckland University of Technology, New Zealand. He is currently a Senior Lecturer with York St John University, U.K. He has more than 23 years of teaching and industry experience. He was a Lecturer, a Senior Lecturer, and an Assistant Professor at a number of reputable universities and private training establishments and have actively involved in the process of teaching, assessment development, moderation, research, training, and curriculum development. He is the New Zealand Qualification Authority's Certified Adult Trainer, a Skilled Assessor, an Expert Moderator, and an Assessment Designer.